Tuning DNA-amphiphile condensate architecture with strongly binding counterions

A. V. Radhakrishnan[a], S. K. Ghosh[a], G. Pabst[b], V. A. Raghunathan[a,1], and A. K. Sood[c]

[a]Raman Research Institute, Bangalore 560 080, India; [b]Institute of Biophysics and Nanosystems Research, Austrian Academy of Sciences, 8042 Graz, Austria; and [c]Department of Physics, Indian Institute of Science, Bangalore 560 012, India

Edited* by Noel A. Clark, University of Colorado at Boulder, Boulder, CO, and approved February 24, 2012 (received for review September 27, 2011)

Electrostatic self-assembly of colloidal and nanoparticles has attracted a lot of attention in recent years, since it offers the possibility of producing novel crystalline structures that have the potential to be used as advanced materials for photonic and other applications. The stoichiometry of these crystals is not constrained by charge neutrality of the two types of particles due to the presence of counterions, and hence a variety of three-dimensional structures have been observed depending on the relative sizes of the particles and their charge. Here we report structural polymorphism of two-dimensional crystals of oppositely charged linear macroions, namely DNA and self-assembled cylindrical micelles of cationic amphiphiles. Our system differs from those studied earlier in terms of the presence of a strongly binding counterion that competes with DNA to bind to the micelle. The presence of these counterions leads to novel structures of these crystals, such as a square lattice and a $\sqrt{3} \times \sqrt{3}$ superlattice of an underlying hexagonal lattice, determined from a detailed analysis of the small-angle diffraction data. These lower-dimensional equilibrium systems can play an important role in developing a deeper theoretical understanding of the stability of crystals of oppositely charged particles. Further, it should be possible to use the same design principles to fabricate structures on a longer length-scale by an appropriate choice of the two macroions.

electrostatic self-assembly | small-angle X-ray scattering | surfactant-DNA complexes

A significant fraction of the counterions of a highly charged macroion, immersed in an aqueous solution, may remain bound to it due to the interplay between electrostatic energy and entropy. This counterion condensation phenomenon depends on the geometry of the macroion and in the case of linear macroions, such as polyelectrolytes, it occurs if the linear charge density is higher than one electronic charge per Bjerrum length, l_B, which is the distance at which the electrostatic energy between two elementary charges is equal to the thermal energy $k_B T$ (1, 2); $l_B \sim 0.7$ nm in water at 25 °C. Two oppositely charged macroions form complexes by releasing these condensed counterions into the aqueous solution and thereby increasing their entropy (3–5). Counterion release has been extensively studied in the context of biomacromolecular association (3, 4). If at least one of these macroions is sufficiently rigid, complexes with ordered structures can result, as in the case of DNA and cationic amphiphiles (6–14). Depending upon the preferred shape of the self-assembled aggregates of the amphiphile, three different structures of these complexes have been found. Bilayer forming cationic lipids form lamellar complexes (L_α^c), with the DNA strands sandwiched between the bilayers (9, 10). An inverted hexagonal (H_{II}^c) complex is obtained if the bilayers are highly flexible or in the presence of "helper lipids" that favor inverted cylindrical micelles (11). The formation of these two structures has been theoretically studied based on the nonlinear Poisson-Boltzmann equation and a phase diagram in the lipid—DNA composition plane has been constructed (12). In addition to the above structures, an intercalated hexagonal (H_I^c) complex has been observed in the case of the cationic amphiphile, cetyltrimethylammonium bromide (CTAB), that self-assembles into cylindrical micelles (13, 14), which is a two-dimensional analogue of crystals of oppositely charged colloidal particles mentioned earlier (15–18).

In this letter we report polymorphic phase behavior of two-dimensional DNA-amphiphile complexes in the presence of strongly binding counterions. Complexes of DNA with cetyltrimethylammonium tosylate (CTAT) and CTAB, and the influence of different salts on the structures exhibited by them were studied using small-angle X-ray scattering (SAXS) techniques. Counterions are known to have a significant effect on the morphology of the amphiphile micelles. For example, CTAT, which has the strongly binding tosylate (T^-) counterion, forms long worm-like micelles (WLM) at a concentration of about 1 wt.% in water (19), whereas CTAB, with the much more weakly binding Br^- counterion, forms shorter cylindrical micelles even at much higher concentrations. However, CTAB can be induced to form WLM if the aqueous solution contains about 100 mM NaBr or KBr (20). Organic salts such as sodium tosylate and sodium salicylate are much more efficient at inducing WLM in CTAB solutions, due to the strongly binding nature of the tosylate and salicylate counterions (21). We show that complexes of DNA with CTAT exhibit three different structures depending on the CTAT and DNA concentrations. The structure found at low CTAT and high DNA concentrations is the H_I^c structure observed earlier in DNA-CTAB complexes. The new architectures are a square (S_I^c) structure seen at low DNA concentrations, and a hexagonal superlattice ($H_{I,s}^c$) structure occurring at high DNA and CTAT concentrations, which is a $\sqrt{3} \times \sqrt{3}$ superlattice of the H_I^c structure. The arrangement of the micelles and DNA in these structures has been determined from a detailed analysis of the diffraction data. The S_I^c structure is found only in the presence of strongly binding counterions, such as T^-, that can compete with DNA to bind to the micelles. On the other hand, formation of the $H_{I,s}^c$ structure requires the presence of WLM, which can be induced even by weakly binding counterions, albeit at relatively higher concentrations. Based on our observations a qualitative explanation of the phase behavior is proposed.

Results and Discussion

The complexes are birefringent under a polarizing microscope indicating the formation of ordered structures. X-ray diffraction studies show the occurrence of three different structures in CTAT-DNA complexes depending upon CTAT and DNA concentrations (Fig. 1). Based on the diffraction data, a partial phase diagram of the system in the ρ-C_s plane has been constructed, where ρ is the surfactant to DNA base molar ratio, and C_s the total CTAT concentration in the solution (Fig. 2). The S_I^c structure seen at low DNA concentrations (high ρ) has a lattice

Author contributions: V.A.R. and A.S. designed research; A.V.R., S.K.G., and G.P. performed research; A.V.R. and V.A.R. analyzed data; and G.P. and V.A.R. wrote the paper.

The authors declare no conflict of interest.

*This Direct Submission article had a prearranged editor.

[1]To whom correspondence should be addressed. E-mail: varaghu@rri.res.in.

This article contains supporting information online at www.pnas.org/lookup/suppl/doi:10.1073/pnas.1115541109/-/DCSupplemental.

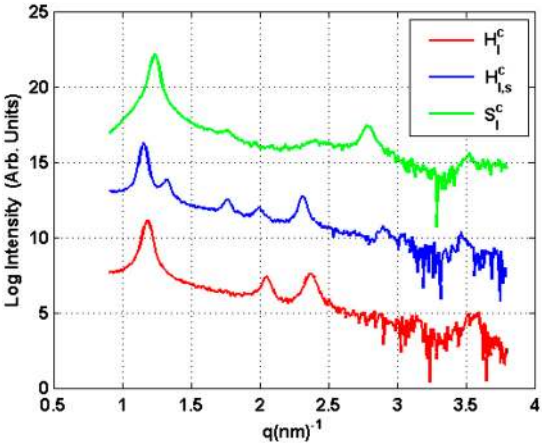

Fig. 1. Diffraction patterns of the three different structures of CTAT-DNA complexes: The square (S_I^c) phase at $C_s = 50$ mM and $\rho = 3.78$ (*Top*), the hexagonal superlattice ($H_{I,s}^c$) phase at $C_s = 90$ mM $\rho = 0.48$ (*Middle*), and the hexagonal (H_I^c) phase at $C_s = 50$ mM, $\rho = 0.50$ (*Bottom*).

parameter $a \sim 5.0$ nm, which is insensitive to both ρ and C_s. In the H_I^c structure seen at high DNA and low CTAT concentrations, $a \sim 5.70$ nm at $C_s = 10$ mM and increases gradually to approximately 6.11 nm at $C_s = 80$ mM; it is, however, rather insensitive to ρ. In the $H_{I,s}^c$ structure observed at high CTAT and DNA concentrations, $a \sim 11.0$ nm. An important aspect of the $H_{I,s}^c$ structure is that the (10) reflection is always absent in its diffraction pattern. Another type of diffraction pattern is observed at very low C_s and high ρ that consists of only two peaks with their spacings in the ratio 1 : 2. Therefore, it was not possible to identify the corresponding structure unambiguously.

Complex formation requires that the oppositely charged moieties in the two macroions be as close to each other as possible. As a result, the structure of the complex usually corresponds to a close-packing of the two macroions. It is possible to propose unique close-packed structures of the square and hexagonal complexes consistent with the values of their lattice parameters and the known diameters of DNA and CTAT micelles. But this is not possible in the case of the super hexagonal structure because of its much larger lattice parameter. In order to arrive at the structures of all three types of complexes we, therefore, adopted a two-step procedure. Assuming the structures to be centrosymmetric, we first calculated electron density maps of the three types of complexes from the diffraction data for all combinations of the phases of the reflections. For each complex only a

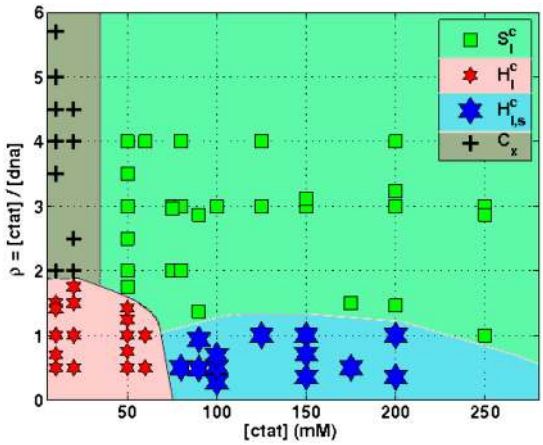

Fig. 2. Partial phase diagram of the complexes determined from diffraction data. H_I^c, S_I^c, and $H_{I,s}^c$ denote the hexagonal, square, and hexagonal superlattice structures, respectively. C_x denotes an unidentified structure which gives only two reflections with their spacings in the ratio 1 : 2.

few of these maps clearly show distinct regions corresponding to the micelles and DNA (Fig.3, *Left*). We then modeled the structures suggested by these maps, by considering the DNA to be discs of radius r_d and uniform electron density ρ_d, and the micelles to be made up of a hydrocarbon core of radius r_c and electron density ρ_c, surrounded by an annular head group region of width δ and electron density ρ_h (14). In the case of the $H_{I,s}^c$ phase, the centers of the micelles occupy special positions, but those of the DNA were varied. Values of some of the model parameters, namely, r_d, ρ_d, ρ_c, and the water electron density ρ_w are available in the literature, and the rest were tuned within reasonable limits to get the best fit of the calculated diffraction data with the observed ones (see *Supporting Information*). This procedure led to a unique structure for each phase.

Structures of the different phases of CTAT-DNA complexes obtained from this procedure are shown in the right panel of Fig. 3. We should stress here that these are not mere schematics. The relative positions of the micelles and DNA, and the micellar size correspond to the best-fit values of the model parameters. The structure of the hexagonal phase is similar to that proposed earlier for CTAB-DNA complexes (13, 14). In this close-packed structure (plane group: *p6m*) each DNA is intercalated between three CTAT micelles, whereas each micelle is surrounded by six DNA. The square phase also has a closed-packed structure (plane group: *p4m*) where the coordination number of both DNA and CTAT micelles is four. The structure of the $H_{I,s}^c$ complex corresponds to a $\sqrt{3} \times \sqrt{3}$ superlattice of the H_I^c structure (plane group: *p6m*). The superlattice formation is associated with the presence of two types of arrangements of the DNA around the micelles. In one of them the 6-fold rotational symmetry present in the H_I^c structure is retained, whereas the other has only threefold symmetry around the micelle. Consistent with this, the best-fit values of the micellar structural parameters, r_c, δ, and ρ_h, are found to be slightly different for the two types of micelles. This structure also reproduces the vanishingly small intensity of the (10) reflection (see *Supporting Information*).

Micellar radii of CTAB and CTAT are comparable, as indicated by the almost identical values of the lattice parameters of their H_I^c complexes with DNA. Therefore, the multiplicity of structures observed in CTAT-DNA complexes, but not in CTAB-DNA complexes, does not result from packing considerations and can be attributed to the tosylate counterion of CTAT. In order to understand the origin of this polymorphism, we have studied the effect of different counterions such as Cl^-, Br^-, and tosylate (T^-) on CTAT-DNA and CTAB-DNA complexes.

The effect of adding NaCl to an aqueous solution containing CTAB-DNA complexes is just to swell the H_I^c structure and dissolve it at [NaCl] ~ 750 mM. Such salt-induced swelling and melting of complexes has been reported in other lipid-DNA systems (22). The melting of the complex at high salt concentration is due to the fact that the counterion release mechanism ceases to work when the ion concentration in the bulk becomes comparable to that near the surfaces of the uncomplexed macroions. On the other hand, the influence of NaT on these complexes is qualitatively different and depends on the CTAB to DNA molar ratio. At high values of $\rho(\sim 4.0)$ the H_I^c phase is transformed into the S_I^c phase at a NaT concentration of approximately 20 nM. On the other hand, at low values of $\rho(\sim 0.5)$, the H_I^c phase is first transformed into the $H_{I,s}^c$ phase at a concentration of about 20 mM and then into the S_I^c phase at a concentration of approximately 40 mM. In both cases the complex dissolves into an isotropic dispersion at [NaT] ~ 100 mM. The much lower NaT concentration required to destabilize the complex compared to NaCl is related to the possibility of charge reversal of the micelles in the presence of T^-. The addition of KBr to CTAB-DNA complexes leads to a $H_I^c \rightarrow H_{I,s}^c$ transformation at a concentration of approximately 300 mM, but the S_I^c structure is not observed in this case. The

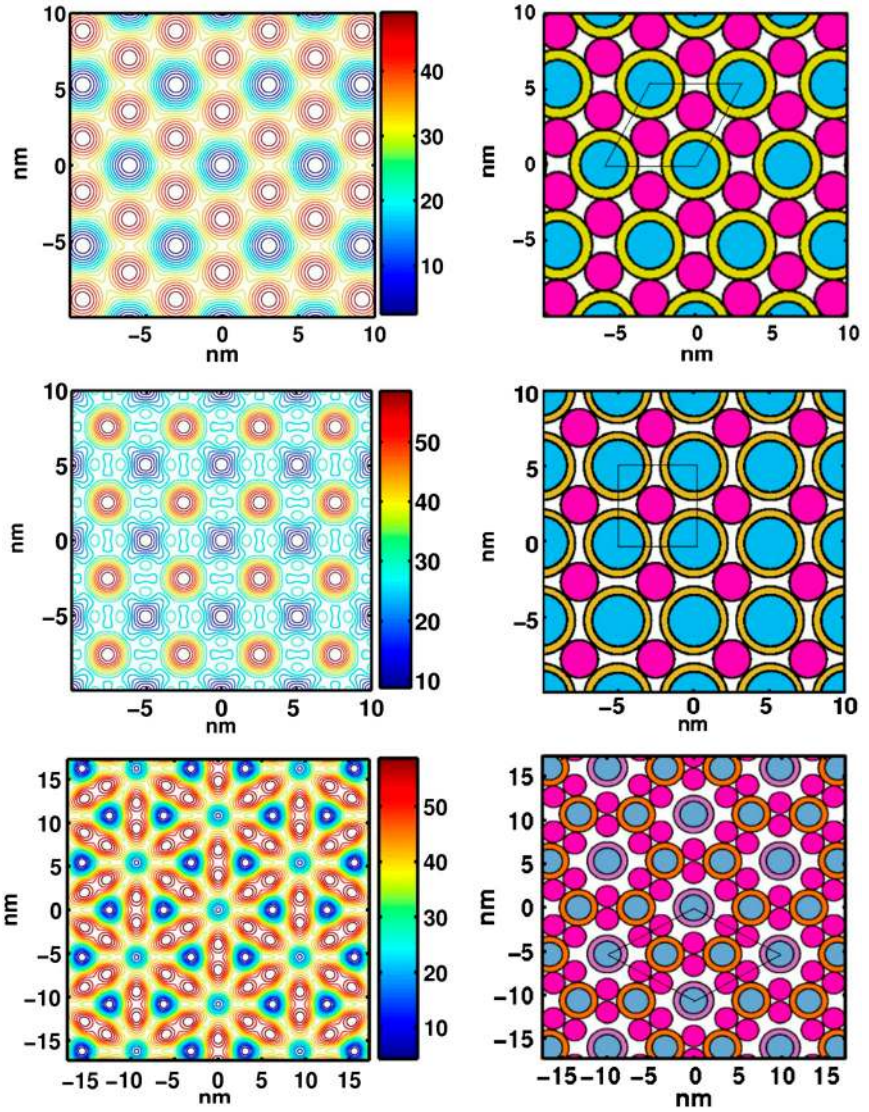

Fig. 3. *Left* shows relative electron density maps of the H_I^c (*Top*), S_I^c (*Middle*), and $H_{I,s}^c$ (*Bottom*) phases of CTAT-DNA complexes, obtained from the diffraction data. The high electron density regions correspond to DNA and the low ones to the hydrocarbon chain region of the micelles. For each structure, maps were constructed for all combinations of the phases of the reflections; the ones shown here were picked as they most clearly show the DNA and micelles making up these structures. Based on these maps, electron density models were constructed for each of these structures, as described in the text. *Right* shows the structures of the corresponding phases obtained from the best-fit values of the model parameters. The red discs correspond to the DNA, the blue ones to the hydrocarbon core of the micelles, and the annular rings to the head group regions. The head group regions are shown in different colors to emphasize differences in their electron densities. The relative positions of the DNA and micelles, and the sizes of the hydrocarbon core and head group region of the micelles are as obtained from the best fit. Note the presence of two types of arrangements of DNA around the micelles in the $H_{I,s}^c$ structure.

complex is ultimately destabilized at a KBr concentration of approximately 500 mM.

Addition of NaCl to the H_I^c phase of CTAT-DNA at $C_s =$ 20 mM leads to a gradual swelling of this phase, with a increasing from 5.75 nm with no salt to 6.29 nm at [NaCl] = 500 mM. As NaCl concentration is further increased, this structure is first converted into $H_{I,s}^c$, and then the complex dissolves forming an isotropic dispersion (I) at [NaCl] ~ 750 mM. Similar $H_I^c \rightarrow H_{I,s}^c \rightarrow I$ transformations are also observed at $C_s \sim 50$ mM. The S_I^c phase observed at higher values of ρ also melts into an isotropic dispersion at around 750 mM NaCl concentration.

The effect of NaT on the S_I^c phase is very similar to that of NaCl, but with the difference that the critical salt concentration at which the complex melts is much lower at around 100 mM. However, the effect of NaT on the H_I^c phase is very different and similar to that observed with CTAB-DNA complexes. It shows the following sequence of transformations with increasing NaT concentration:

$$H_I^c \overset{\sim 50\ \mathrm{mM}}{\rightarrow} H_{I,s}^c \overset{\sim 75\ \mathrm{mM}}{\rightarrow} S_I^c \overset{\sim 100\ \mathrm{mM}}{\rightarrow} I.$$

The occurrence of the $H_{I,s}^c$ phase in between H_I^c and S_I^c suggests an alternative noncentrosymmetric structure of this phase. In the H_I^c phase the coordination number of the micelle is 6, whereas in the S_I^c phase it is 4. If we take the coordination number to be 5 in the $H_{I,s}^c$ phase, then we can come up with the structure shown in Fig. 4, which is obtained by removing one of the six DNA strands surrounding each micelle. This leads to a hexagonal vacancy superlattice, whose lattice parameter is comparable to that obtained from the diffraction data. We have, therefore, modeled this structure and compared the calculated diffraction data to the observed ones. The best-fit values are given in the *Supporting Information*. We find that this model is not consistent with the diffraction data, the quality of the fit being very much poorer than for the structure shown in Fig. 3. Further, the intensity of the (10) reflection could not be made negligible for any

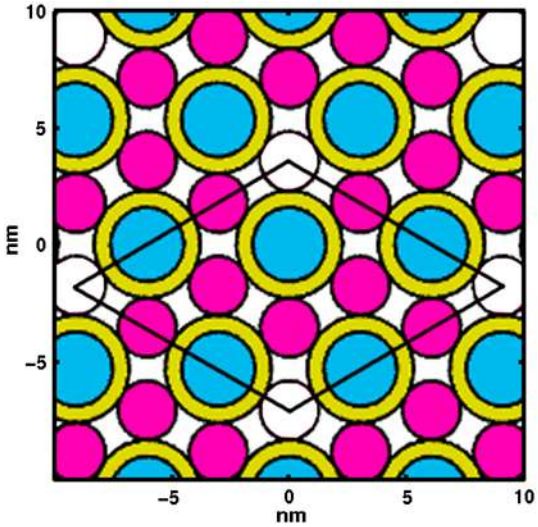

Fig. 4. A noncentrosymmetric structure of the $H^c_{I,s}$ phase suggested by the salt-induced phase changes of CTAT-DNA complexes. The empty circles denote missing DNA strands. Note that these vacancies form a hexagonal superlattice, whose lattice parameter is comparable to that obtained from the diffraction data.

reasonable values of the model parameters. We can, therefore, rule out this structure for the $H^c_{I,s}$ phase.

On the basis of the proposed structures we can understand the observed polymorphism of CTAT-DNA complexes. As mentioned earlier, the tosylate counterion is much more strongly bound to the micelles due to its hydrophobic toluene moiety than Br^-. This leads to a competition between the counterion and DNA to bind to the micelle. At low DNA content it is possible to bind all the DNA to the micelles in the S^c_I phase, with minimal release of the T^- ion, since this structure has one DNA strand per micelle. From this stoichiometric ratio, the value of ρ in this structure can be estimated to be approximately 3.0, so that up to this value of ρ all the DNA can be incorporated in the complex, since its chemical potential in the S^c_I phase is lower than that in the aqueous solution. As ρ is decreased below 3, the H^c_I complex is formed at $\rho \sim 1.5$, which can incorporate twice the amount of DNA compared to the S^c_I structure, as it has two DNA per micelle. We do not observe the coexistence of the S^c_I and H^c_I structures in any of the samples, which is consistent with the phase rule, according to which such a coexistence should be confined to a line in the ρ-C_s plane. As ρ is further decreased, the lattice parameter of the H^c_I structure initially decreases slightly, due to the thinning of the micelles in order to incorporate some additional DNA. Beyond this point no more DNA can be incorporated in the complex.

With increasing C_s at a fixed ρ, more and more NaT is released as a result of complexation. The increasing T^- concentration in the solution leads to a higher degree of adsorption on the micellar surface, resulting in a weaker binding of the DNA to the micelles. In the case of the S^c_I structure this does not lead to the swelling of the complex, except probably in a narrow concentration range just before the complex dissolves. On the other hand, a gradual swelling of the H^c_I structure is observed with increasing NaT concentration. However, beyond a point this uniformly swollen state becomes unstable and decomposes into two types of micellar environments, resulting in the superlattice ($H^c_{I,s}$) structure. With further increase in the salt concentration, achieved either by the addition of NaT or by increasing C_s, the S^c_I phase is obtained, which can incorporate more T^- ions in the micelles. Further increase in T^- concentration leads to a greater adsorption of the counterion on the micelle, which eventually destabilizes the complex leading to an isotropic dispersion.

From our observations we can conclude that the formation of the S^c_I structure requires the presence of a counterion that can compete with DNA to bind to the micelle, since we find it only with T^- (23). On the other hand, the $H^c_{I,s}$ structure is formed in systems that support the formation of WLM, such as CTAT, CTAT + NaCl, CTAB + NaT and CTAB + KBr. Our earlier studies on amphiphile-polyelectrolyte complexes indicate that the morphology of the amphiphile aggregates in the complex is closely related to that in the corresponding amphiphile-water system at amphiphile concentrations comparable to that in the complex (24). The structure of the $H^c_{I,s}$ phase given in Fig. 3 shows that one set of micelles is in a local environment that is relatively water-rich. Therefore, it is very likely that only a WLM forming system can support such a structure.

The main objective of this article has been to show that the competition between the counterion and DNA to bind to the micelle can lead to novel structures of DNA-amphiphile complexes. In the past, spontaneous curvature and flexibility of the amphiphile aggregates have been demonstrated to be crucial factors in determining the structure of these complexes (11). Our work demonstrates conclusively that a strongly binding counterion can also be used to tune the structures of these systems. The superlattice structure found in these experiments is not close-packed and can be at least partially stabilized by the entropy of the micelles. Although entropic stabilization is a well-known phenomenon in colloidal crystals, it has not been considered so far in theoretical investigations on the energetics of amphiphile-DNA complexes. We feel that the incorporation of these two features, namely, presence of a competing species and entropic stabilization, is very important for a deeper understanding of the stability of complexes of oppositely charged particles.

Materials and Methods

CTAB, CTAT, sodium salt of calf thymus DNA, NaCl, KBr, and sodium tosylate (NaT) were obtained from Sigma-Aldrich. All chemicals were used as received. Complexes were prepared by adding appropriate amounts of DNA to amphiphile solutions in deionized water (Millipore). Complexes, along with some of the supernatant, were taken in 1 mm diameter glass capillaries for X-ray diffraction studies, which were carried out either using a rotating anode generator (Rigaku, UltraX-18) fitted with a multilayer focusing mirror (Xenocs) and an image plate detector (Marresearch), or a SAXSeye small-angle scattering system (Hecus). Higher resolution data from a few samples were collected using the SAXS beamline at the Elettra synchrotron source, Trieste, Italy.

ACKNOWLEDGMENTS. We thank Rema Krishnaswamy for discussions and Bibhu Ranjan Sarangi for help in conducting the synchrotron experiments. A.K.S. thanks CSIR, India, for support through a Bhatnagar fellowship.

1. Manning GS (1969) Limiting laws and counterion condensation in polyelectrolyte solutions. *J Chem Phys* 51:924–933.
2. Le Bret M, Zimm BH (1984) Distribution of counterions about a cylindrical polyelectrolyte and Manning's condensation theory. *Biopolymers* 23:287–312.
3. Record MT, Anderson CF, Lohman TM (1978) Thermodynamic analysis of ion effects on the binding and conformational equilibria of proteins and nucleic acids. *Q Rev Biophys* 11:103–178.
4. Sharp KA, Friedman RA, Misra V, Hecht J, Honig B (1995) Salt effects on polyelectrolyte-ligand binding: Comparison of Poisson-Boltzmann and limiting law/counterion binding models. *Biopolymers* 36:245–262.
5. Wagner K, et al. (2000) Direct evidence for counterion release upon cationic lipid—DNA condensation. *Langmuir* 16:303–306.
6. Felgner PL, et al. (1987) Lipofection: A highly efficient, lipid-mediated DNA-transfection procedure. *Proc Natl Acad Sci USA* 84:7413–7417.
7. Felgner PL, Rhodes G (1991) Gene therapeutics. *Nature* 349:351–352.
8. Bruinsma R (1998) Electrostatics of DNA—cationic lipid complexes: Isoelectric instability. *Eur Phys J B* 4:75–88.
9. Radler JO, Koltover I, Salditt T, Safinya CR (1997) Structure of DNA—cationic lipid complexes: DNA intercalation in multilamellar membranes in distinct interhelical packing regimes. *Science* 275:810–814.
10. Lasic DD, Strey H, Stuart MCA, Podgornik R, Frederik PM (1997) The structure of DNA—liposome complexes. *J Am Chem Soc* 119:832–833.

11. Koltover I, Salditt T, Radler JO, Safinya CR (1998) An inverted hexagonal phase of cationic liposome—DNA complexes related to DNA release and delivery. *Science* 281:78–81.
12. May S, Ben-shaul A (2004) Modeling of cationic lipid—DNA complexes. *Curr Med Chem* 11:151–167.
13. Krishnaswamy RVA, Raghunathan VA, Sood AK (2004) Reentrant phase transitions of DNA-surfactant complexes. *Phys Rev E* 69:031905.
14. Krishnaswamy R, Pabst G, Rappolt M, Raghunathan VA, Sood AK (2006) Structure of DNA—CTAB—hexanol complexes. *Phys Rev E* 73:031904.
15. Leunissen ME, et al. (2005) Ionic colloidal crystals of oppositely charged particles. *Nature* 437:235–240.
16. Bartlett P, Campbell AI (2005) Three-dimensional binary superlattices of oppositely charged colloids. *Phys Rev Lett* 95:128302.
17. Kalsin AM, et al. (2006) Electrostatic self-assembly of binary nanoparticle crystals with a diamond-like lattice. *Science* 312:420–424.
18. Shevchenko EV, Talapin DV, Kotov NA, O'Brien S, Murray CB (2006) Structural diversity in binary nanoparticle superlattices. *Nature* 439:55–59.
19. Soltero JFA, Puig JE, Manero O, Shultz PC (1995) Rheology of cetyltrimethylammonium tosylate—water system. 1. Relation to phase behavior. *Langmuir* 11:3337–3346.
20. Candau SJ, Hirsh E, Zana R (1984) New aspects of the behaviour of alkyltrimethylammonium bromide micelles: light scattering and viscosimetric studies. *J de Phys* 45:1263–1270.
21. Berret JF (2005) Rheology of worm-like micelles. *Molecular Gels*, eds R Weiss and P Terech (Elsevier, Dordrecht), pp 235–275.
22. Koltover I, Salditt T, Safinya CR (1999) Phase diagram, stability, and overcharging of lamellar cationic lipid—DNA self-assembled complexes. *Biophys J* 77:915–924.
23. Similar behavior has also been found with salicylate counterion, which is also strongly-binding.
24. Krishnaswamy R, Mitra P, Raghunathan VA, Sood AK (2003) Tuning the structure of surfactant complexes with DNA and other polyelectrolytes. *Europhys Lett* 62:357–362.